Astron. Astrophys. 59, 43—52 (1977)

ASTRONOMY AND ASTROPHYSICS

Aperture Synthesis Observations of Galactic H II Regions

V. The Galactic Nebula S 252 (NGC 2175)

M. Felli[1], H. J. Habing[2] and F. P. Israël[2]

[1] Osservatorio di Arcetri, Largo E. Fermi 5, 50125 Firenze, Italy
[2] Sterrewacht, Leiden, The Netherlands

Summary. Aperture synthesis observations at 1415 and 4995 MHz and fan beam observations at 408 MHz of the galactic diffuse nebula NGC 2175 are presented.

A comparison of the radio structures with the Hα surface brightness distribution indicates the presence of several thermal components located at the edge of a low density ($n_e \approx 10\,\mathrm{cm}^{-3}$) extended H II region. The main source of ionization is the O 6.5V star HD 42088. The large scale optical and radio emission is bounded by an ionization front on the west side, while it is density bounded on the east side. Of the four thermal small diameter components of higher electron density present in NGC 2175, at least two require an internal source of ionization.

An unresolved radio component, with no optical counterpart, is also found in the central part of the optical nebulosity. Based on its spectral index, the radio source can be classified as extragalactic.

A schematical model for the region is derived which agrees with the "blister" model proposed for Orion by Zuckerman (1973), and Balick et al. (1974), for NGC 2024 by Grasdalen (1974) and for S 206 by Deharveng et al. (1975). This is confirmed by a recently discovered CO cloud west of the nebula.

Key words: H II regions — radio observations — NGC 2175

1. Introduction

This paper is part of a series dealing with high resolution observations of galactic H II regions using the Westerbork Synthesis Radio Telescope (WSRT) (Israël et al., 1973; Israël, 1976a, 1976b, 1976c).

The galactic diffuse nebula NGC 2175 is a good example of an H II region containing complex structures. The optical nebula has a size of 25′ and is characterized by dust lanes, bright rims and bright condensations, all embedded in a fainter diffuse emission. The region is S 252 in the Sharpless (1959) Catalogue of H II regions and is in the class of the brightest objects. A stellar cluster is associated with the nebulosity (Pismis, 1970), with an estimated age of $2\,10^6$ years (Grasdalen and Carrasco, 1975). The O 6.5V star HD 42088, located approximately at the centre of the nebula, is undoubtedly one of the main sources of ionization of the H II region. As a (thermal) radio source it is known as W 13 from the catalogue by Westerhout (1958). The nebula has been suggested for observation to radioastronomers by Osterbrock (1968) at a Symposium on H II regions.

We present aperture synthesis observations of the entire nebula at 1415 MHz and of two selected fields at 4995 MHz, made with the WSRT. The high angular resolution and sensitivity of this instrument allowed us to detect several small diameter radio components inside the extended radio emitting region. These components were not detected in previous radio observations of NGC 2175; they are of interest for a detailed comparison of the optical and the radio structure of the region and lead to a better understanding of the processes going on inside the nebula.

The parameters of the diffuse extended region were derived from fan beam observations at 408 MHz taken with the East-West arm of the Bologna Radio Telescope.

A short review of previous radio observations and optical information on the exciting stars is given in Section 2.

The synthesis observations at 1415 and 4995 MHz and those at 408 MHz are described in Section 3, where the derived parameters are also given.

In Section 4 the radio and the optical structure are compared and the various components are analyzed.

Section 5 contains a general discussion of the H II region with particular emphasis on the nature of one bright condensation (S 252-a) and on the range of cloud masses contained in the region.

Send offprint requests to: M. Felli

Table 1. Low resolution radio observation of NGC 2175

Frequency	Flux density (f. u.)	Diameter (′)	Ref.
178 MHz	19	15±8	Bennet (1963)
243	44±8	—	Terzian (1965)
405	51±5	—	Terzian (1965)
610	27±2	—	Dickel et al. (1967)
750	39±5	—	Terzian (1965)
750	31.3	—	Pauliny Toth et al. (1966)
750	29.4±3	18	Höglund (1967)
1400	29.1	—	Pauliny Toth et al. (1966)
1410	35.2±4	—	Höglund (1967)
1410	43±3	—	Terzian (1965)
2700	28	19	Day et al. (1972)
4170	35	31	Kaifu and Morimoto (1969)
4995	30	—	Gebel (1968)

Table 2. Distance determinations of NGC 2175

Method	Distance (kpc)	Ref.
Hα slit spectrograph	2.4	Miller (1968)
H 158α line radial velocity	2.87	Dieter (1967)
Distance of HD 42088	1.91	Georgelin (1975)
Brightest star in the cluster	1.95	Pismis (1970)

2. Review of Available Information on NGC 2175

The centre of the optical nebulosity is at $\alpha = 06^h\,06^m$ and $\delta = 20°\,30'$ (1950.0); its galactic coordinates are $l = 190.0°$ and $b = 0.5°$. The region is thus located in the direction of the anticentre, where galactic background emission is of minor importance.

Previous low resolution radio observations of this region are given in Table 1. The main conclusions derived from these observations can be summarized as follows:

a) The radio source has approximately the same position and size as the optical nebula.

b) The only indication of structure is a weak depression in the centre of the source (Terzian, 1965).

c) The spectrum can be fitted with an optically thin free-free spectrum, down to at least 405 MHz. Thus NGC 2175 is a region with a low emission measure and therefore a low r.m.s. electron density.

We note that the source 3C 153.1 at $\alpha = 06^h\,06^m\,42^s$ and $\delta = 21°\,12'$ ($\pm 24'$), $S_{178\,\mathrm{MHz}} = 19$ f.u. (Bennet, 1963) has been identified erroneously with the bright small component S 252a inside NGC 2175 (Wyndham, 1966) and should instead be associated with the whole nebula. The radio east-west diameter of 3 C 153.1 is in fact $15 \pm 8'$.

No 4 C source is reported in this area, which implies the absence of small diameter sources with $S_{178\,\mathrm{MHz}} \geqq 2$ f.u. in the observed field.

The radio source has also been observed with higher resolution (HPBW = 2′) at 15 GHz by Churchwell and Felli (1969). They detected the presence of structure on the scale of the beamsize in the central part of the nebula, containing in total about 0.72 f.u.

Two aperture synthesis observations have been reported in the literature. The first by Balick (1972) was performed at 8 GHz and at 2.9 GHz and was centered on the bright condensation S 252a. No radio emission was found at the position of the optical feature, down to a flux level of 10 m.f.u., while a point source with a flux density of 40 m.f.u. was detected in the 2.9 GHz map, approximately 15.5 s west and 5′.5 north of HD 42088. This source was outside the field of view of the 8 GHz map.

The other synthesis observation is by Felli et al. (1974) and is only an east-west stripscan, positioned on the centre of NGC 2175. The source was detected only marginally, i.e. with flux density $\lesssim 0.5$ f.u. at 10 GHz. It was concluded that some flux may be contained in scale sizes of the order of 0′.5 or less.

Several independent determinations of the distance of NGC 2175 are listed in Table 2. In the following we shall adopt for the whole nebula $D = 2$ kpc, the photometric distance of the star HD 42088.

The main source of ionization of the H II region detected optically is the star HD 42088, with a spectral type O 6.5 V (Conti and Alschuler, 1971; Walborn, 1972). Other blue stars in the nebulae have been studied by Garnier and Lortet-Zuckermann (1971), who give for the blue star close to the "globule" S 252a a spectral type between O 8 and B 0.5, and by Grasdalen and Carrasco (1975), who find several stars of spectral types between BOV and B 7 and assign a spectral type B 1V to the star close to S 252a.

Two stellar clusters are present in this region of the sky. One is centered on the nebulosity (called NGC 2175), the other, of smaller dimension (called NGC 2175s) is located on the north east of the nebula. According to Pismis (1970), the stars in the larger cluster (NGC 2175) are distributed in a spherical shell. The reddening varies from $E_{B-V} = 0.7$ for NGC 2175s to $E_{B-V} = 0.2$ to 0.3 m for the larger cluster. The proximity of the two clusters is then interpreted as a projection effect. The distances found from the brightest star in each cluster place them at 3500 pc (NGC 2175s) and 1900 pc (NGC 2175), respectively.

3. Observations and Data Reduction

The 1415 MHz observations were obtained with the WSRT in a single 12^h measurement. For a description of the instrument and of the receivers we refer to Baars and Hooghoudt (1974) and to Casse and Muller (1974). The minimum spacing between antennas was 36 m, the other spacings being increments of 72 m. The half power widths of the central part of the synthesized antenna pattern are 24″ in right ascension and 70″ in declination.

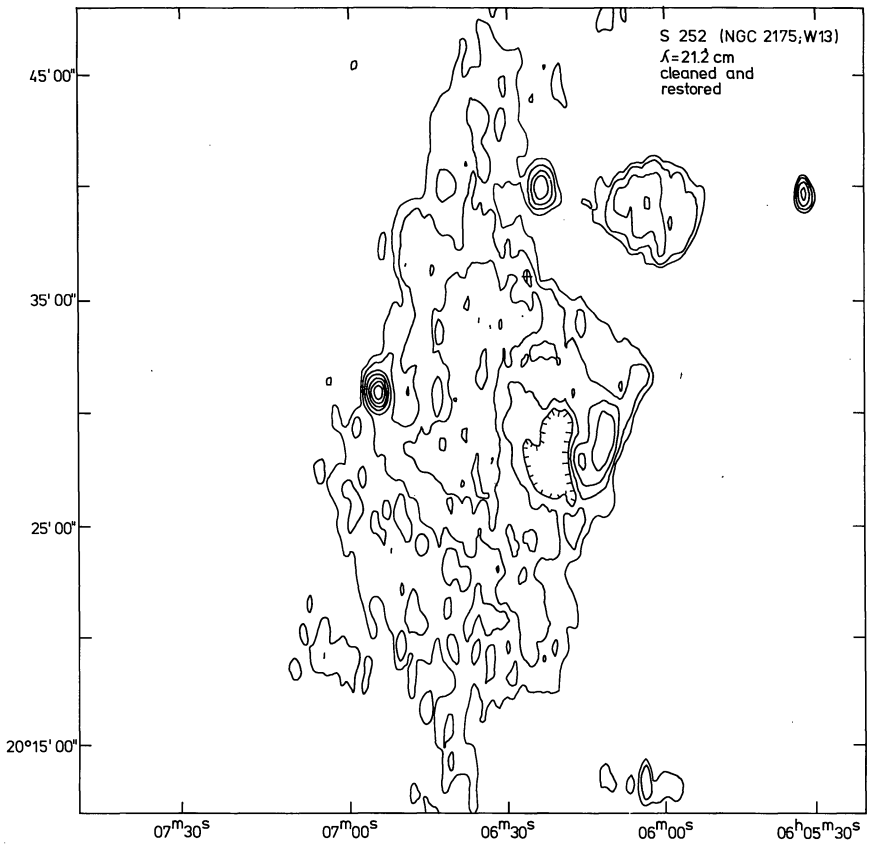

Fig. 1. Contour map of NGC 2175 at 21 cm continuum. Contour values are 4, 7.5, 15, 25, 37.5, 50, 62.5 and 75 m.f.u. per synthesized beam. Component *D* has been subtracted from the map; its position has been indicated by a cross

Standard calibration and reduction procedures were used (Högbom and Brouw, 1974; van Someren Greve 1974).

The map derived directly by Fourier Transform of the (u, v) data showed the presence of several small diameter sources and of an extended diffuse region. The interferometric pattern resulting from the 12^h synthesis is composed of the central part just described, surrounded by grating ellipses at intervals of 10′ in right ascension and of a central "bowl" depression of about 10′ diameter. The depression results from the absence of interferometer spacings less than 36 m. As a consequence sources and their interferometric responses are mutually overlapping in the original map and may produce reduction problems for very extended and complex regions. This confusion was eliminated with the use of the Clean-Restore procedure (Högbom, 1974; Harten, 1976).

The map was cleaned down to a level of 5 m.f.u. per synthesized beam area.

The cleaned-restored map, uncorrected for the single dish antenna pattern is shown in Figure 1. The contours indicate lines of constant flux density per synthesized beam area. One m.f.u. per synthesized beam of $24 \times 70''$ corresponds to a brightness temperature $T_b = 1.1$ K.

The most noticeable features in the map are an extended weak component, called E_{1415}, and six small diameter sources, called *A* to *F* as indicated in Figure 2. To obtain better resolution maps of these small diameter components and to be able to make a spectral identification it was decided to reobserve the components *A* to *E* at 4995 MHz.

Since the field of view of the WSRT at 4995 MHz is smaller than at 1415 MHz, we observed two fields with a 12^h synthesis centered at:

$\alpha = 06^h06^m00^s \quad \delta = 20°39'36''$

and

$\alpha = 06^h06^m38^s \quad \delta = 20°33'00''$

The surface brightness of the extended component was too weak at this frequency to be detected in the maps.

The analysis of the data was performed in a way similar to that indicated for the 1415 MHz data.

The observed parameters of the various components and the two frequencies are listed in Table 3. The coordinates given in Columns 2 and 3 refer to the peak of the sources. The observed east-west and north-south gaussian diameters were derived from crosscuts through the peak positions. The values in Table 3 are corrected for finite beamwidth using a gaussian deconvolution.

The flux densities were determined by planimetering the contours and are corrected for the effect of the primary beam. The errors in the flux densities quoted

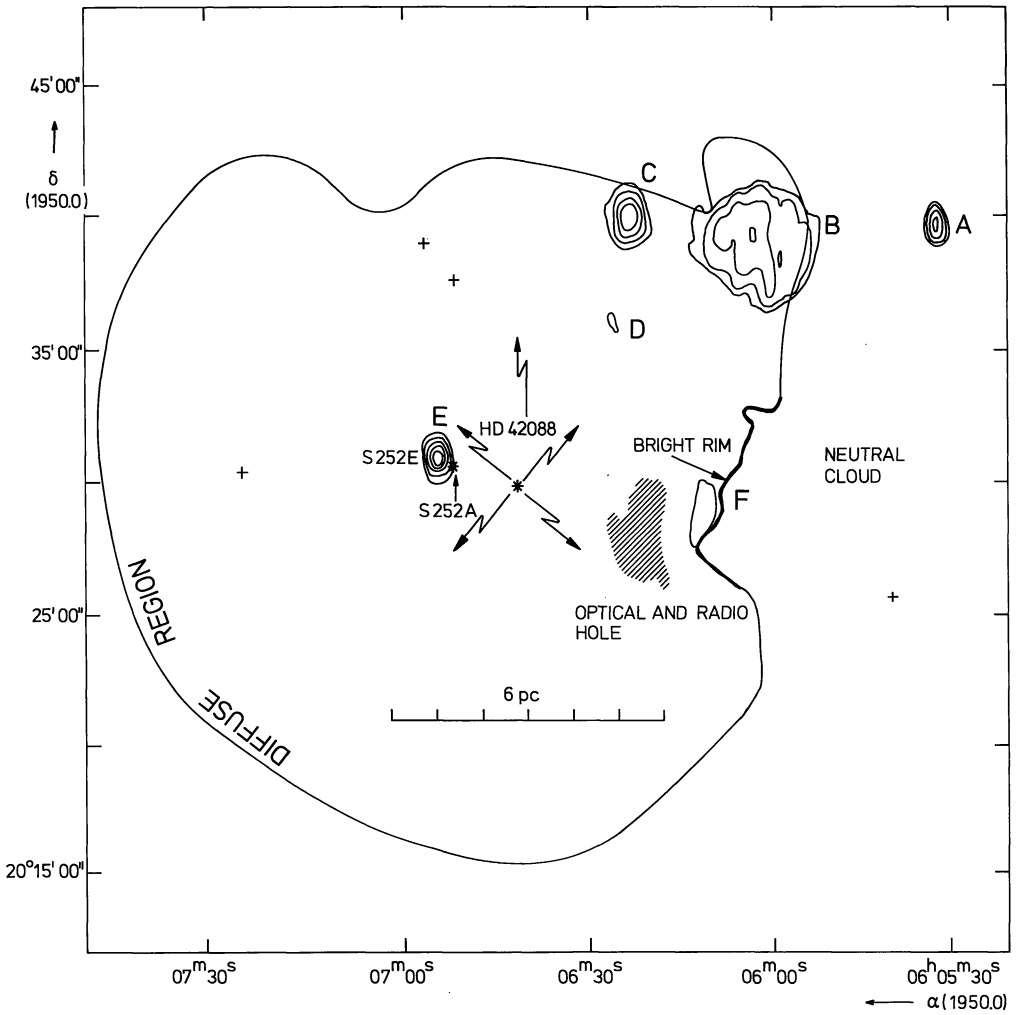

Fig. 2. Sketch of the most important features in the NGC 2175 region. The four crosses are reference stars used for the overlay. The contour "Diffuse Region" is a sketch of the outer edge of the nebulosity

are caused mainly by the uncertainty in the background level.

For the extended component E_{1415} the interpretation of the observed parameters requires more attention. Since the minimum spatial frequency sampled by the interferometer was 36 m/λ, components with sizes $\gtrsim 10'$ are attenuated in the synthesized map. This explains why the diameter of E_{1415} (measured from the half power contours) is only 6′ in right ascension as compared to 40′, the size of the optical nebula and why the flux density contained in E_{1415} is only 6 f.u., compared to the value of about 30 f.u. measured by low resolution radio telescopes.

The source E_{1415} describes therefore only the more intense structures in the extended region; the lower intensity diffuse features are lost in the synthesis map. The flux density contained in the small diameter structure is only $\approx 10\%$ of the total flux density.

To study in more detail the radio emission associated with the diffuse emission we used observations at 408 MHz of source BGE 0606+20 (Felli et al., 1977). The observations were made with the East-West arm of the Italian Northern Cross Radiotelescope. The HPBWs of the fan beam are 4′.2 in right ascension and 1.9° in declination, which allows a good angular description of the source structure in right ascension while it integrates in declination. At this frequency and with such a wide beam the instrument is very sensitive to the extended low surface brightness region and the major contribution to the observed radio flux density comes from the diffuse part of NGC 2175.

Scans taken at constant declination through the source are shown in Figure 3. None of the small diameter features detected in the 1415 and 4995 MHz map can be seen in the plots at 408 MHz. The main characteristic at this frequency and resolution is a smooth extended emission region, slightly asymmetrical with a sharp drop at the west side and a smooth decrease on the east side.

The half-power width in right ascension is $\theta_{408} = 20 \pm 1'$. This is only a lower approximation to the true source diameter for sources with a very smooth surface

Table 3. S 252 Observed parameters

Component	Equatorial Coordinates α (1950.0)	δ (1950.0)	Galactic coordinates l	b	Flux density S_{1415} (f. u.)	S_{4995} (f. u.)	Angular diameter α (′)	δ (′)	Quadratic mean
(1)	(2)	(3)	(4)	(5)	(6)	(7)	(8)	(9)	(10)
A Total	$06^h05^m33^s$	20°39′50″	189.77	0.34	0.230±0.020	0.205±0.050	0.44	0.54	0.49
*A*1	06 05 31.6	20 39 34	—	—	—	0.025±0.005	0.13	0.27	0.19
*A*2	06 05 32.6	20 39 48	—	—	—	0.055±0.010	0.17	0.30	0.23
*A*3	06 05 33.7	20 39 47	—	—	—	0.130±0.030	0.30	0.50	0.40
B Total	06 06 02	20 39 11	189.83	0.43	1.40 ±0.60	0.800±0.150	4.2	4.2	4.2
C Total	06 06 23	20 40 07	189.86	0.51	0.160±0.030	0.120±0.030	0.60	0.60	0.60
*C*1	06 06 22.2	20 40 13	—	—	—	0.025±0.005	0.12	0.07	0.09
*C*2	06 06 23.2	20 40 03	—	—	—	0.045±0.015	0.25	0.37	0.30
*C*3	06 06 24.3	20 40 08	—	—	—	0.035±0.010	0.12	0.23	0.17
*C*4	06 06 25.1	20 39 48	—	—	—	0.015±0.005	0.05	0.37	0.14
D	06 06 25.3	20 35 28	189.93	0.48	0.200±0.030	0.070±0.010	<0.05	<0.07	<0.06
E Total	06 06 54	20 30 55	190.05	0.54	0.150±0.030	0.145±0.050	0.60	0.32	0.44
*E*1	06 06 53.6	20 30 45	—	—	—	0.060±0.020	0.30	0.60	0.42
*E*2	06 06 54.3	20 30 40	—	—	—	0.025±0.010	0.08	0.16	0.11
*E*3	06 06 55.2	20 30 55	—	—	—	0.015±0.005	0.10	0.10	0.10
*E*4	06 06 56.1	20 31 15	—	—	—	0.010±0.005	0.15	0.10	0.12
F	06 06 11	20 29 02	190.00	0.38	0.600±0.200	—	1.65	0.60	1.0
E_{1415}	06 06 30	20 45	190	0.5	6	—	6	—	6
E_{408}					44.2*	—	45	—	45

* At 408 MHz.

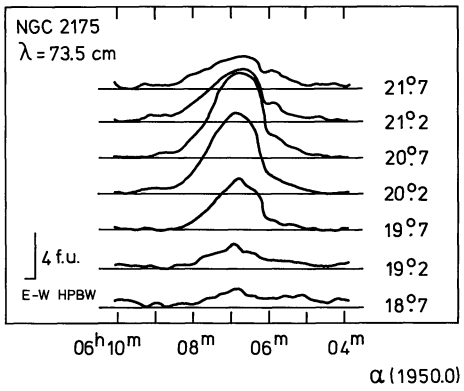

Fig. 3. Fan beam scans at constant declination of NGC 2175 at 408 MHz. The vertical bar in the lower left corner is the deflection of a point source of 4 f.u., while the horizontal bar is the East-West equivalent beam width

brightness decrease at the edges. If we measure the distance between the two extreme points where the deflection is greater than 0.6 f.u. on the most intense East-West scan of Figure 3, we obtain $\theta'_{408}=45'.6$. This is an upper limit to the source diameter and is slightly larger than the optical diameter (40′) on the red print of the Palomar Sky Survey.

The integrated flux density at 408 MHz is 44.2 f.u. This number includes the contribution of the diffuse extended component and of the six small diameter components found at 1415 MHz. However, the contribution of the small components (*A* to *F*) to the total flux density is less than 10%, of the same order as the error involved in the 408 MHz measurement. In the following we shall assume 44.2 f.u. as representative of the flux density of the extended component E_{408}, with 45′ as the angular diameter.

For each of the components in Table 3 (except for component *D*) we determined the r.m.s. electron density (n_e), the mass of ionized hydrogen ($M_{HII}/M_\odot$), the emission measure (E.M.), and the excitation parameter (u). We used the relations given by Mezger and Henderson (1967), in the homogeneous cylindrical approximation. The electron temperature was assumed to be equal to $T_e=10^4$ K. The use of these relations implies the assumption that the components are all optically thin at 1415 and 4995 MHz.

The derived quantities, based on a distance of 2 kpc, are listed in Table 4. Identification of the thermal nature of these components is based on the spectral index between 1415 and 4995 MHz and on their correspondence with Hα features.

For the extended component both the parameters at 1415 MHz and at 408 MHz were derived with the understanding that E_{1415} is representative of the inner more intense part, while E_{408} represents the contribution from the entire nebula.

4. Observational Results on Individual Components

The Hα photograph of NGC 2175 shown in Figure 4, was kindly provided by Lortet-Zuckermann. This

Table 4. S 252 derived model physical parameters[a]

Component (1)	Mean diameter d(pc) (2)	r.m.s. electron density n_e(cm^{-3}) (3)	Peak emission measure E.M. (10^4 pc cm^{-6}) (4)	Ionized mass M ($M_\odot$) (5)	Excitation parameter u(pc cm^{-2}) (6)
A Total	0.34	550	10.4	0.4	13
*A*1	0.12	795	8.5	0.04	
*A*2	0.16	885	12.7	0.07	
*A*3	0.28	595	9.9	0.25	
B Total	2.9	45	0.6	21	21
C Total	0.42	310	4.1	0.4	11
*C*1	0.06	2440	38	0.01	
*C*1	0.21	540	6.1	0.10	
*C*3	0.12	1110	14.8	0.04	
*C*4	0.10	975	9.3	0.02	
E Total	0.31	545	7.5	0.3	12
*E*1	0.29	375	4.1	0.18	
*E*2	0.08	1805	25	0.02	
*E*3	0.07	1615	18.3	0.01	
*E*4	0.08	1000	8.5	0.01	
F	0.7	300	6.4	2.0	18
E_{1415}	4.2	65	1.8	95	39
E_{408}	31	9	0.2	5200	76

[a] Assumed distance $D=2$ kpc; assumed electron temperature $T_e=10^4$ K

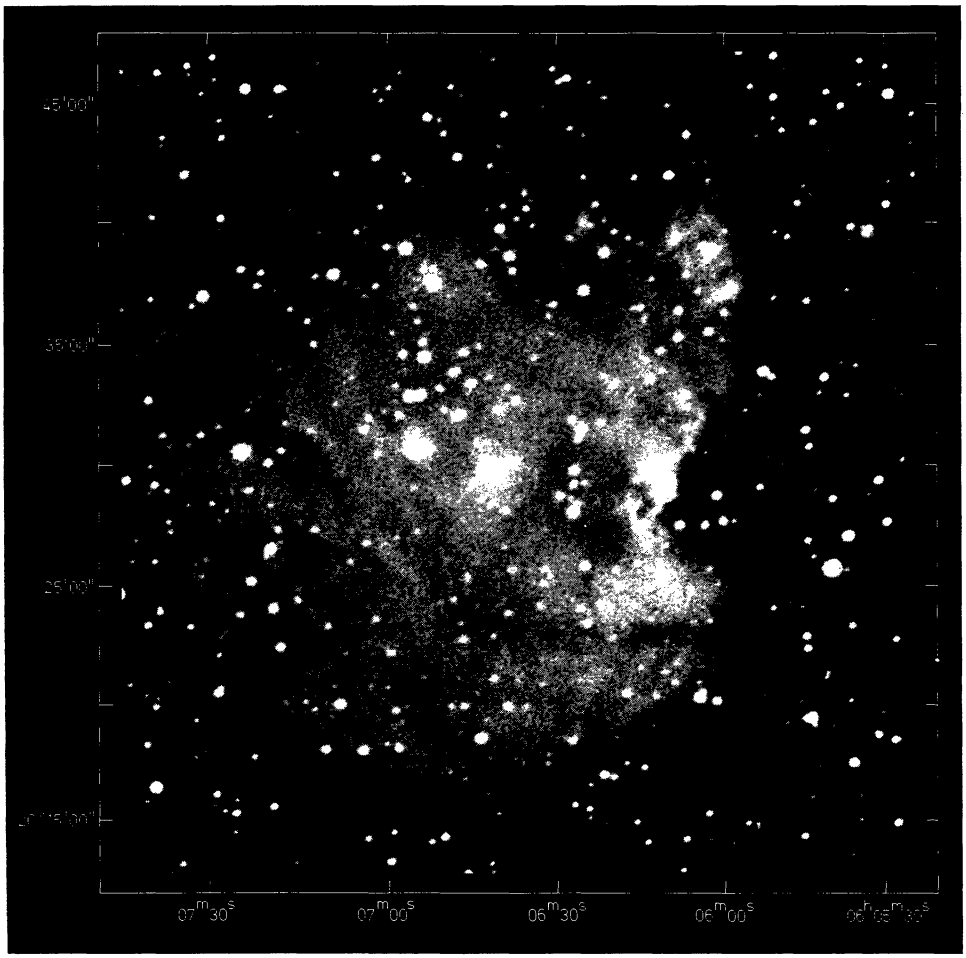

Fig. 4. Hα photograph of NGC 2175 (Courtesy M. C. Lortet-Zuckerman)

photograph is the basis for the comparison between radio components and the Hα surface brightness. We now discuss the results of this comparison.

1. The Extended Components E_{1415} and E_{408} ($l=190°, b=0°.5$)

The radio contours at 1415 MHz agree well with the bright features over the entire nebula. In particular the following comments can be made:

a) The very sharp bright rim at the western edge of the nebula is well represented both in the radio contours at 1415 MHz and in the 408 MHz scans. Source *F* may be considered as the brightest part of the extended emission. The close correspondence of this bright optical rim on the west side with component *F*, implies that the rim is not due to foreground obscuration, but that it is a true ionization front. This implies the existence of an extended neutral cloud on the western side of NGC 2175. At our request, G. Baran searched for CO emission near S 252. He indeed found a cloud with a size of about 35′ (corresponding to 20 pc) west of the nebula, centered on $\alpha=06^h05^m30^s$ and $\delta=29°40'$.

b) No radio feature with a flux density >5 m.f.u. is coincident with the exciting star HD 42088 either in the 1415 or the 4995 MHz map.

c) The decrease of the optical surface brightness between HD 42088 and the ionization front (source *F*) is also well represented in the radio map, which implies that this is a real large scale variation in the projected electron density distribution and not an obscuration effect. The minimum is not centered on HD 42088 but is about 4′ to the west.

d) The radio emission decreases smoothly on the east side of the nebula. This is particularly evident in the 408 MHz profile at $\delta=21°$ and is in agreement with the gradual decrease of the optical surface brightness. The H II region thus may be density bounded on this side. The excitation parameter of the O 6.5V star HD 42088, $u=62.8$ pc cm^{-2} (Panagia, 1973) and the observed excitation parameter for the entire extended region ($u_{408}=73$) coincide within the experimental errors. No other stars are required for the ionization of the nebula and HD 42088 is therefore very probably the main source of ionization of the nebula.

e) Very notable is a gradual increase in electron density towards the ionization front (component *F*). The very extended E_{408} component has an r.m.s. electron density of only 9 cm^{-3}, the smaller component E_{1415} already has 65 cm^{-3}, while the rim area *F* yields an r.m.s. electron density of 300 cm^{-3}. Thus a density gradient towards the interface with the neutral cloud is clearly present.

2. Component A ($l=189°.77, b=0°.34$)

This small diameter component coincides with a bright patch of nebulosity on the Hα photograph, separated from the more extended nebulosity. The Lyman photon-flux falling on this component from the star HD 42088 is computed assuming that the projected distance is equal to the true distance between the two objects. This flux falls at least an order of magnitude short of the amount needed for its excitation, hence a local source of ionization is required. At 6 cm (see Fig. 5) the source is resolved, and presents a sharp edge on the east side. The object consists of several dense clumps (cf. Table 4). On the blue print of the Palomar Sky Survey a star can be clearly seen in the centre of the nebulosity.

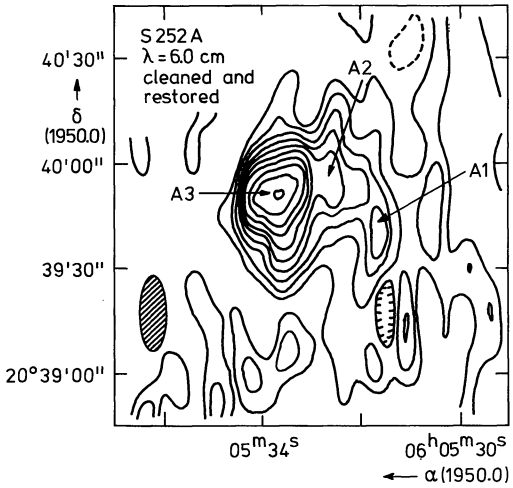

Fig. 5. Contour map of component *A* at 4995 MHz. The map was cleaned and restored. Contour values are 1 to 10 f.u.m. per synthesized beam area, in steps of 1 m.f.u. per synthesized beam area

3. Component B ($l=189°.83, b=0°.43$)

While on the optical photograph this component might be considered as part of the main nebulosity, the radio map of Figure 1 shows that this is an individual source, on top of weak background emission. The correspondence between the three brightest optical features and the radio contours is very good; some finer structure is present in this component. However, no dense components are present in this nebula, that gives the impression of a well-evolved object. A thermal spectrum for this component is compatible with the quoted errors on the flux density. Since component *B* is an extended source of low surface brightness the 4995 MHz flux may be a lower approximation to the true one. The Lyman photon-flux from HD 42088 falls short about a factor two to explain the observed excitation parameter. The star LSV +20°16 (Garnier and Lortet-Zuckermann, 1971) lies exactly in the centre of component *B* (see Fig. 6). Its spectral type according to Grasdalen and Carrasco (1975) is B 2V and hence it cannot account for the observed excitation parameter. A further search for the source of ionization (or more accurate spectral classification) is therefore necessary.

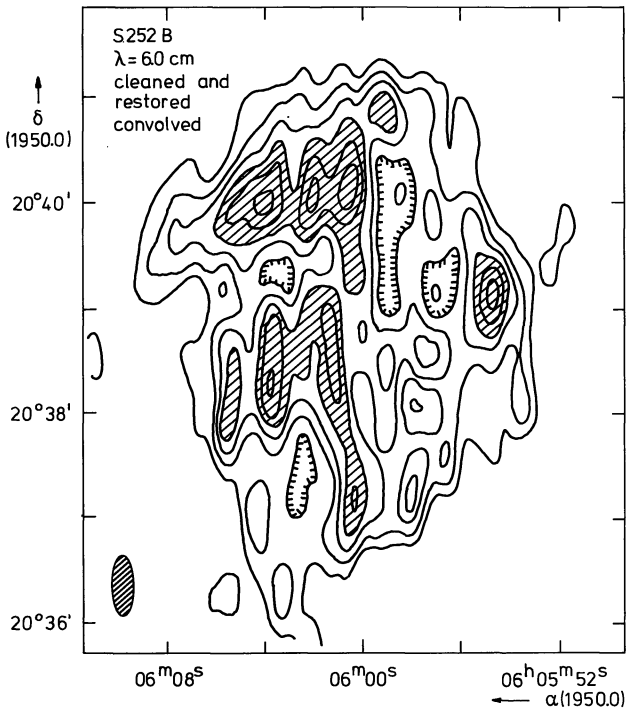

Fig. 6. Contour map of component *B* at 4995 MHz. The map was convolved to a beam 12.5 × 33.″9; subsequently cleaned and restored. Contour values are 2.5 to 15 m.f.u. per synthesized beam area in steps of 2.5 m.f.u. per synthesized beam area. Areas within the 10 m.f.u. contour have been dashed

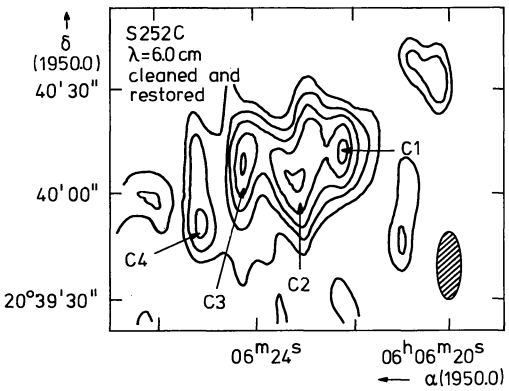

Fig. 7. Contour map of component *C* at 4995 MHz. The map was cleaned and restored. Contour values are 1 to 5 m.f.u. per synthesized beam area in steps of 1 m.f.u. per synthesized beam area

4. *Component C* ($l = 189.^{\circ}86$, $b = 0.^{\circ}51$)

This component is well resolved both at 1415 MHz and 4995 MHz (see Fig. 7) and coincides with a small bright patch of nebulosity. The excitation from HD 42088 is about one order of magnitude less than the observed value. It consists of a few very dense clumps, that are embedded in a weaker envelope. It should be remarked that all three components *A*, *B* and *C* are close (within 10′ or 6 pc) from the CO peak.

5. *Component D* ($l = 189.^{\circ}93$, $b = 0.^{\circ}48$)

This is the only unresolved source in the whole field of view (both at 1415 and at 4995 MHz) and also the only one which does not have an optical counterpart. From the 1415 and 4995 MHz flux density it follows that this source is probably extragalactic. Balick (1972) gives a flux density of 40 m.f.u. at 2695 MHz. Since the source was at the edge of Balick's field of view the value might be an underestimate. No polarization is present in the 1415 MHz observation at the position of component *D* down to a level of two percent. The spectral index is $\alpha_{4995}^{1415} = -0.8$. Extrapolation of the flux density of component *D* to 178 MHz with this spectral index would give a source of ≈1 f.u. At the position of *D*, no source is present in the 4 C catalogue. Absorption by the foreground nebulosity NGC 2175 yields an optical depth of only 0.05 at 178 MHz.

6. *Component E* ($l = 190.^{\circ}05$, $b = 0.^{\circ}54$)

The component coincides with a small bright nebulosity, studied optically by Garnier and Lortet-Zuckerman (1971). We will call this nebulosity S 252E. No radio emission was found by Balick (1972) at 2695 MHz. This is surprising considering the derived flux density at 1415 MHz and 4995 MHz (0.15 f.u.), and the stated sensitivity of Balick's observations (0.01 f.u.).

The radio source has a diameter of 0.′6, smaller than that of the optical nebulosity (1 × 2′). This might be an effect of overexposure of the optical photograph and implies an increase of the column density towards the centre. The bright knot contains two blue stars, visible only on short exposures, which are not centered with respect to the globule but shifted towards the northwest. The strongest of the two will be called S 252a. Photometric and spectroscopic observations of S 252a by Garnier and Lortet-Zuckermann (1971) indicate a spectral type between O 8 and B 0.5, while according to Grasdalen and Carrasco (1975) the type is B 1 V. The corresponding range of excitation parameters is very wide, between 7.3 and 37.4 pc cm^{-2} (Panagia, 1973); and the observed value $u = 11$ pc cm^{-2} falls in between. Derivation of a detailed ionization balance of this component is not possible with the present uncertainties. Ionization from HD 42088 cannot be excluded since, at the projected distance, the Lyman photon-flux from this star is of the same order as that implied by the radio emission. S 252E was also observed in the near-infrared by Zeilik (1976). From the radio observations, one would predict S (2.2 μm) = 0.04 f.u., whereas Zeilik finds S (2.2 μm) = 0.51 f.u. Thus the ionized gas contributes only a small percentage of the total near-infrared brightness. The rest is probably due to very hot dust. This implies that a hot local star is required and suggests that S 252a is indeed the exciting star of S 252E, rather than HD 42088. The 4995 MHz map (see Fig. 8) shows S 252E to contain a number of

dense clumps. One of them (E 1) gives the impression of being a bright rim structure; it is also the brightest clump in the source.

7. *Component F* ($l=190^{\circ}.00$, $b=0^{\circ}.38$)

As pointed out in the discussion of the extended component, the separation of source *F* from the background emission in the 1415 MHz map is somewhat artificial. This source cannot be considered an individual component as the previous ones, but rather the region of highest surface brightness of the extended component, coincident with the ionization front which separates the H II region produced by the star HD 42088 and the cloud of neutral material.

The observed excitation parameter is in complete agreement with the Lyman photon-flux emitted by HD 42088 in the solid angle subtended by component *F*.

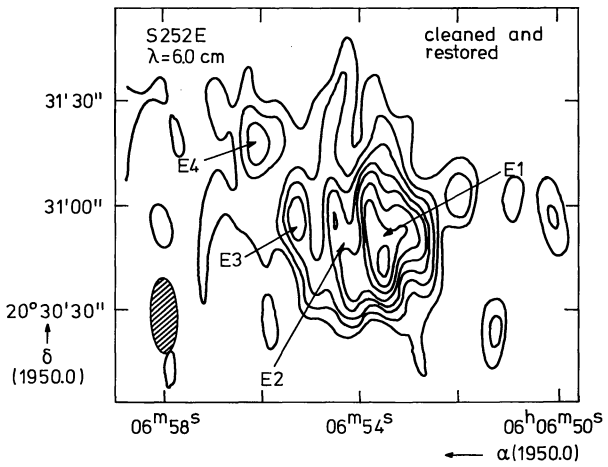

Fig. 8. Contour map of component *E*(S 252E) at 4995 MHz. The map was cleaned and restored. Contour values are 1 to 8 m.f.u. per synthesized beam area in steps of 1 m.f.u. per synthesized beam area

5. Discussion

The picture that emerges from the preceding analysis of the individual components suggests the co-existence of objects with different characteristics and possibly different natures.

i) A low density extended H II region, ionized by the O 6.5V star HD 42088, located approximately at its baricentre. The contribution to the ionization of the other stars of the cluster (for which the spectral type is known) is negligible in comparison to that of HD 42088. On the western side the region is characterized by an extended ionization front. On this side the region is bounded by a neutral massive cloud with a size comparable to the size of NGC 2175 itself, as shown by CO observations. A possible explanation of the gradual decrease of the surface brightness (radio and optical) and of the implied electron density decrease towards the eastern side of the front is that hot ionized gas (constantly supplied during the slow erosion of the neutral cloud produced by the ultraviolet radiation of HD 42088) streams away from the ionization front. The three-dimensional "blister" model of the Orion Nebula by Zuckerman (1973) and by Balick et al. (1974) seems to be well applicable in this case, with the advantage that in NGC 2175 we are seeing the exciting star and the ionization front from aside. Presence of other ionization fronts in the region is suggested by the non-uniform distribution of the diffuse emission.

The low density ($n_e=9\ \mathrm{cm}^{-3}$) and the linear size ($d\approx 30$ pc) of the extended region places it in the class of evolved H II regions (Churchwell, 1974; Israël, 1976c). It is well known (see e.g. Spitzer, 1968) that as an H II region expands the Strömgren radius varies and $n_e^{-2/3}$ and hence the total ionized mass proportional to n_e^{-1} increases as the gas expands. If the extended region represents an advanced phase in the evolution of the H II regions, the derived mass will not be related to the mass of the protostellar cloud that originated HD 42088 but rather to the mass of the whole cloud of which the protostellar cloud was one of the subcondensation that succeeded in forming a star (although this gas has expanded considerably). With regard to the total mass of the original cloud, the mass of the early type stars that ultimately formed appears to be only a small fraction.

ii) Components *A*, *B* and *C* appear to be individual and independent H II regions of higher surface brightness, probably excited internally by stars of spectral type later than of HD 42088. They are located near the edge of the extended source, component *A* being the more distant one. The higher densities of these regions with respect to the extended source and the requirement of being internally excited suggest that they may be in an earlier phase of evolution with respect to the extended component. Their location close to the CO peak is suggestive.

iii) The bright optical component S 252E has been extensively studied in the optical domain. Two slightly different explanations for the nature of S 252E are given. According to Garnier and Lortet-Zuckermann (1971), this is a young compact H II region ionized by the blue star S 252a. Grasdalen and Carrasco, on the basis of a strong optical continuum emission attributed to scattered light, argue that the star S 252a must be located at the edge of a neutral high density globule, ionizing it from the outside.

In the preceeding paragraph we have shown that if the projected distance between S 252E and HD 42088 is the true distance, then the ultraviolet radiation from HD 42088 can fully account for the observed radio emission. Since, however, S 252a is so close to S 252E and appears to influence its shape (see Fig. 8) and since S 252E shows strong near-infrared emission it is likely that S 252a is the ionizing star of S 252E. Hence the proximity of S 252E to HD 42088 might be a projection

effect only and S 252E may actually be located at the far end of the nebula. A new independent determination of the spectral type of S 252a seems necessary to resolve the contradictory statements made by Grasdalen and Carrasco (1975) and by Garnier and Lortet-Zuckerman (1971).

It is wortwhile to notice that three (possibly four) thermal components found in the region of NGC 2175 are near the edge the extended component, even assuming the projected distance to be the real one. A similar phenomenon has been found by Harten (private communication) in NGC 7822. This may indicate that secondary star formation is influenced by the presence of a well developed H II region. The star cluster associated with the nebulosity shows a similar spherical distribution with no central condensation (Pismis, 1970).

iv) The occurence of an extragalactic source in the field (component *D*) simply tells us that in the analysis of radio emission from H II regions, observations at two frequencies are necessary to allow to separate spurious background sources from H II regions.

The overall picture that emerges from the observations of the NGC 2175 complex is that of a hierarchy of masses and densities in the evolution of H II regions: very massive clouds at low densities, which can be detected as H II regions only in the very late stages of the evolution, represent the large scale clouds within which star formation may occur. Lower mass and higher density components (which may contribute only a small portion of the total continuum flux density) are instead more closely connected with the subcondensations from which the stars originated.

Acknowledgements. We thank M. Spermon for actively taking part in the reduction of the WSRT observations. M. C. Lortet-Zuckerman kindly drew our attention to this object and provided the Hα photograph. We thank G. Grasdalen for providing his observational results prior to publication and G. Baran for kindly supplying us with the relevant CO data.

We also wish to express our appreciation to Dr. D. Harris, Dr. N. Panagia and Dr. G. Tofani for critically reading the manuscript.

The radio observations could only be made with the helpful assistance of the Westerbork Telescope Group, headed by J. B. Bregman and the Leiden Reduction Group headed by H. W. van Someren Gréve.

The Westerbork Synthesis Radio Telescope is operated by the Netherlands Foundation for Radio Astronomy which is financially supported by the Netherlands Organisation for the Advancement of Pure Research (Z.W.O.).

References

Baars, J. W. H., Hooghoudt, B. C.: 1974, *Astron. Astrophys.* **31**, 323
Balick, B.: 1972, *Astrophys. J.* **176**, 353
Balick, B., Gammon, R. H., Hjellming, R. M.: 1974, in H II regions and the Galactic Centre, 8th ESLAB Symposium, ed. A. F. M. Moorwood, ESRO SP-105
Bennet, A. S.: 1963, *Monthly Notices Roy. Astron. Soc.* **127**, 3
Casse, J. L., Muller, C. A.: 1974, *Astron. Astrophys.* **31**, 333
Churchwell, E., Felli, M.: 1969, *Astron. J.* **75**, 69
Churchwell, E.: 1974, in Proceedings of the Second European Regional Meeting in *Astron. Mem. Soc. Astron. Ital.* **45**
Conti, P. S., Alschuler, W. R.: 1971, *Astrophys. J.* **170**, 325
Day, G. A., Caswell, J. L., Cooke, D. J.: 1972, *Australian J. Phys. Suppl.* **11**, 25
Deharveng, L., Israël, F. P., Maucherat, M.: 1976, *Astron. Astrophys.* **48**, 63
Dickel, J. R., Yang, K. S., Mc. Vittie, G. C., Swenson, G. W.: 1967, *Astron. J.* **72**, 757
Dieter, N. H.: 1967, *Astrophys. J.* **150**, 435
Felli, M., Tofani, G., D'Addario, L. R.: 1974, *Astron. Astrophys.* **31**, 431
Felli, M., Tofani, G., Fanti, C., Tomasi, A.: 1977, *Astron. Astrophys. Suppl.* **27**, 181
Garnier, R., Lortet-Zuckerman, M. C.: 1971, *Astron. Astrophys.* **14**, 408
Gebel, W. L.: 1968 *Astrophys. J.* **153**, 743
Georgelin, Y.: 1975, Ph. D. thesis, Université de Provence, Obs. de Marseille
Grasdalen, G. L.: 1974, *Astrophys. J.* **193**, 373
Grasdalen, G. L., Carrasco, L.: 1975, *Astron. Astrophys.* **43**, 259
Harten, R. H.: 1976 (in preparation)
Höglund, B.: 1967, *Astrophys. J.* **153**, 743
Högbom, J. A.: 1974, *Astron. Astrophys. Suppl.* **15**, 417
Högbom, J. A., Brouw, W. N.: 1974, *Astron. Astrophys.* **33**, 289
Israël, F. P., Habing, H. J., de Jong, T.: 1973, *Astron. Astrophys.* **27**, 143
Israël, F. P.: 1976a, *Astron. Astrophys.* **48**, 193
Israël, F. P.: 1976b, *Astron. Astrophys.* (in press)
Israël, F. P.: 1976c, Thesis, Leiden University
Kaifu, N., Morimoto, H.: 1969, *Publ. Astron. Soc. Japan* **21**, 203
Mezger, P. G., Henderson, A. P.: 1967, *Astrophys. J.* **147**, 471
Miller, J. S.: 1968, *Astrophys. J.* **151**, 473
Osterbrock, D. E.: 1968, Interstellar Ionized Hydrogen, ed. Y. Terzian, W. A. Benjamin, Inc.
Panagia, N.: 1973, *Astron. J.* **78**, 929
Pauliny Toth II, K., Wade, C. M., Heeschen, D. S.: 1966, *Astrophys. J. Suppl.* **13**, 65
Pismis, P.: 1970, *Bol. Obs. Tonantzintla Tacubaya* **5**, 219
Sharpless, S.: 1959, *Astrophys. J. Suppl.* **4**, 257
Someren Greve, H. W. van: 1974, *Astron. Astrophys. Suppl.* **15**, 343
Spitzer, L. Jr.: 1968, Diffuse matter in space, Interscience Publishers
Terzian, Y.: 1965, *Astrophys. J.* **142**, 135
Walborn, N. R.: 1972, *Astron. J.* **77**, 312
Westerhout, G.: 1958, Bull. of the Astr. Inst. of the Netherlands, XIV, 215
Wyndham, J. D.: 1966, *Astrophys. J.* **144**, 459
Zeilik, M.: 1976, *Astron. Astrophys.* **46**, 319
Zuckerman, B.: 1973, *Astrophys. J.* **183**, 863